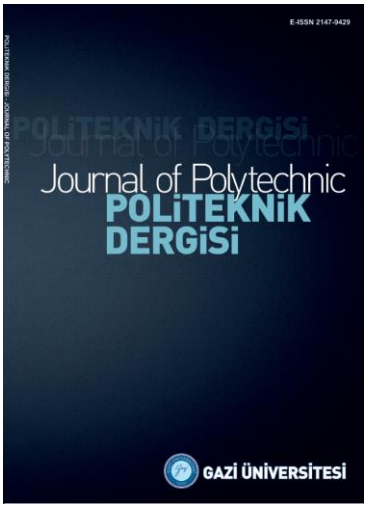

POLİTEKNİK DERGİSİ

JOURNAL of POLYTECHNIC

ISSN: 1302-0900 (PRINT), ISSN: 2147-9429 (ONLINE)
URL: http://dergipark.gov.tr/politeknik

The techno-economic and environmental analysis of a der system in a practical radial distribution feeder under load uncertainty conditions

Belirsiz yük koşullarında bir dek sisteminin pratik radyal dağıtımlı besleyicide tekno-ekonomik ve çevresel analizi

***Yazar(lar) (Author(s))**: Muhammet Tahir GÜNEŞER[1], Abdulbari Ali Mohamed FREI[2]*

ORCID[1]: 0000-0003-3502-2034

ORCID[2]: 0000-0002-7134-2951

To cite to this article: Frei A. ve Güneşer M. T., "The techno-economic and environmental analysis of a der system in a practical radial distribution feeder under load uncertainty conditions", ***Journal of Polytechnic***, 26(2): 731-741, (2023).

Bu makaleye şu şekilde atıfta bulunabilirsiniz: Frei A. ve Güneşer M. T., "The techno-economic and environmental analysis of a der system in a practical radial distribution feeder under load uncertainty conditions", ***Politeknik Dergisi***, 26(2): 731-741, (2023).

Erişim linki (To link to this article): http://dergipark.gov.tr/politeknik/archive

DOI: 10.2339/politeknik.1030685

The Techno-Economic and Environmental Analysis of a DER System in a Practical Radial Distribution Feeder under Load Uncertainty Conditions

Highlights

- *Utilize several mathematical models of Distributed Energy Resource for analyzing the influence on distribution network*
- *Approve the smart distribution network that could give security for process*
- *Proper utilization of the distributed energy resource with the novel organization and smart calculation technologies*
- *Identify optimal positions and ratings of various DERs in distribution network using multi objective crow search optimization technique*
- *Impact on active power purchase, real and reactive power loss, emission generation and voltage deviation analyze after DERs inclusion*

Graphical Abstract

The graphical abstract of the proposed method is shown in following figure.

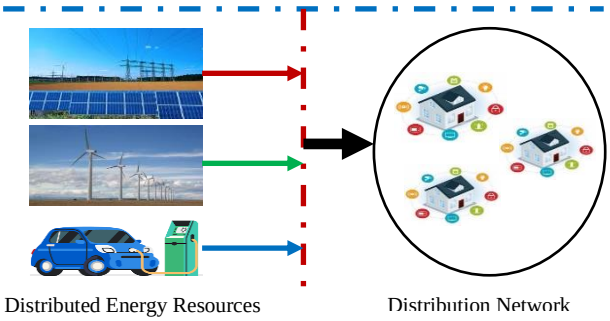

Figure. Graphical Abstract

Aim

The aim of this paper is the following matters under load uncertainty condition: Identify optimal positions and ratings of various DERs in distribution network using multi objective crow search optimization technique.

Design & Methodology

In this paper, we utilized several mathematical models of Distributed Energy Resource for analyzing the influence on distribution network under undefined power demand of one day. Furthermore, the charge and discharge concept of Electrical Vehicle during off-peak and peak hours of the grid has also been taken into contemplation.

Originality

This thesis approved the smart distribution network that could give security for process and proper utilization of the distributed energy resource with the novel organization and smart calculation technologies.

Findings

In this paper, three different distributed energy resources aggregators considerd to interconnect with the Distribution Management System. Electrical vehicle, Wind turbine and solar photovoltaic system will implement and test to distributed energy resource.

Conclusion

In this paper an optimal integration of Distributed Energy Resource (DER) such as Photo-Voltaic Generation System (PVGS), Wind Turbine Generation System (WTGS), and Electric Vehicles (EVs) in supply network simultaneously done for motive of abatement of overall power loss, overall cost and emanations dispatched through the thermal generators.

Declaration of Ethical Standards

The author(s) of this article declare that the materials and methods used in this study do not require ethical committee permission and/or legal-special permission.

Belirsiz Yük Koşullarında Pratik Radyal Dağıtımlı Besleyicide DER'lerin Tekno-Ekonomik ve Çevresel Faydaları

Araştırma Makalesi / Research Article

Muhammet Tahir GÜNEŞER, Abdulbari Ali Mohamed FREI*

Department of Electrical and Electronics Engineering Karabuk University, Karabük, Türkiye

(Geliş/Received : 30.11.2021 ; Kabul/Accepted : 13.12.2021 ; Erken Görünüm/Early View : 10.02.2022)

ÖZ

Bu makale, Rüzgar Enerji Santralleri (RES), Elektrikli Araçlar (EV'ler) ve Fotovoltaik Güneş Enerji Santralleri (FVGES) gibi çeşitli Dağıtılmış Yenilenebilir Enerji Kaynaklarının (DEK'ler) şebekeye mümkün olan en uyumlu şekilde yüklenmesini ve aynı zamanda işletme giderlerini, ısıl jeneratörler tarafından üretilen kirliliği ve toplam şebeke güç kaybını azaltmayı tartışmaktadır. Bu planlanmış hedeflere ve faydalara ulaşmak için çok amaçlı bir işlev yapılandırılmıştır. Bu çalışmada, 24 saatlik bir süre boyunca değişen yük talepleri altında dağıtım enerji sistemi üzerindeki etkiyi analiz etmek için Dağıtılmış Enerji Kaynaklarının farklı hesaplama modelleri kullanılmıştır. Ayrıca, dağıtılmış şebekenin yoğun olmayan/yoğun olduğu saatlerde elektrikli otomobillerin boşaltma/şarj modeli de dikkate alınmıştır. DEK şebekelerinin kabarık olmayan ve süreksiz yapısı nedeniyle, sistemin optimizasyonu için çok amaçlı Karga Arama Algoritması kullanılmıştır.

Anahtar Kelimeler: Dağıtım sistemi, dağıtılmış enerji kaynakları, emisyon, karga arama algoritması, güç kaybı.

The Techno-Economic and Environmental Analysis of a DER System in a Practical Radial Distribution Feeder under Load Uncertainty Conditions

ABSTRACT

This paper discusses the best possible incorporation of various Distributed Renewable Energy Resources (DERs), such as Wind Turbine Generation Systems (WTGS), Electric Vehicles (EVs), and Photo-Voltaic Generation Systems (PVGGS) in distribution networks at the same time in order to reduce overall expense, pollution produced by thermal generators, and total grid power loss. A multiple goal function is structured to achieve these planned goals and benefits. Different computational models of DERs were used in this study to analyze the impact on the distribution energy system under varying load demands over a 24 hour period. Furthermore, the discharging/charging model of electric cars during off peak/peak hours of the distributed grid was taken into consideration. Because of its robustness, the multi objective crow search algorithm was used to optimize the non-bulgy and non-continuous optimization of the distributed energy grid.

Keywords: Distribution system, distributed energy resources, emission, crow search algorithm, power loss.

1. INTRODUCTION

By the end of 2025, DERs are expected to account for 25% of the European Union's (EU) total power consumption [1]. Furthermore, EVs have often been used as a backup power source during peak hours of the distributed energy grid, and they have proven to be effective in reducing oil consumption and noxious waste pollution [2]. Because of their superior energy efficiency and environmental benefits over traditional cars, the future of electric vehicles seems bright [3].

In [4], a variant of the particle swarm optimization method (PSO) algorithm was used to incorporate different forms of distribution generation using green energy resources into the distribution network in order to reduce distribution losses and increase voltage levels. A meta-heuristic programming approach was proposed by [5] to decide upon the optimum positions and sizes of PV arrays and WTs in a ring distribution scheme to reduce power losses and increase voltage levels. In a deterministic distribution network planning problem, the Mixed Integer Non-linear Programming approach was followed by Atwa and El-Saadany [6] to allocate wind-based DGs optimally.

Recently, many studies have been performed to minimize the power consumption [7][8][9][10][11] in the machining [12] of different kinds of materials. And several studies have been proposed about optimization for balancing and sizing supplying resources and demand activities [13][14][15].

*Sorumlu Yazar (Corresponding Author)
e-posta : freiabd@gmail.com

In [16][17], solar energy and wind turbines were used to evaluate the energy in renewable energy systems based on the convolutional neural network.

The integrated objective (Multi-Objective) crow search algorithm was used in this study to solve a multi-objective based optimization task involving the implementation of DERs in distribution networks. This optimization strategy has previously been shown to be effective in a variety of power system activities, including transmission network extension preparation, economic load dispatch, and unit commitment, among others. This gives the author the courage to use it to solve the distribution scheme dilemma. In this paper, a new multi-objective function has been developed to find the best positions for DERs in the delivery feeder, as well as the best quantities of DERs, under load uncertainty. The foraging life of a crow in its seeking food source locations in the available search space inspired this meta-heuristic approach. It is efficient, has a high convergence speed, and is capable of handling complex nonlinear control functions with fewer controlling parameters. Because of these advantages, it has been selected as a preferred method to resolve this problem. This issue has a number of objectives, including lowering overall cost, total real power loss and emissions generated by thermal generators, as well as lowering the voltage level and voltage deviation under load uncertainty. The novel ideas of the manuscript can be presented as follows for better detail:

To check the current, power loss and voltage of the distribution feeder, a backward-forward (B-F) load run method was developed.

To calculate the likelihood of solar irradiance and wind speed, the photovoltaic generation system (PVGS) and WTGS numerical models were used in order to assess predictable production power. Furthermore, the principles of EV discharging and charging are considered in this work. In addition, the authors' contribution in this paper deals with the following subjects under load varying conditions:

Using a multi-objective crow search optimization strategy, we find the best positions and scores for various DERs in the distribution chain.

Various prices, such as successful power procurement, WTGS and PVGS Observations and Measurements (O&M), and installation costs, have been assessed in addition to the cost of EV charging and discharging.

The impact on active power purchase, reactive and active power loss and voltage divergence and emission generation have been analyzed after DERs inclusion.

The remainder of this manuscript is divided as follows: In Section 2, a suggested numerical problem formulation is discussed, which includes a multi-objective function as well as operational constraints. Section 3 discusses the statistical simulation of multiple DERs as well as the discharging/charging principle of EVs over a 24-hour period. Section 4 presents an overview of the multi-objective crow search algorithm and how to use it to solve the problem of optimum DER positioning. In Section 5, the results of the simulation and a discussion on the results are presented. Section 6 of the report contains the conclusions.

2. PROPOSED NUMERICAL PROBLEM FORMULATION

Due to environmental issues and the system's varying load requirements, a consideration has been suggested for the implementation of different DERs in the delivery system. As a result, a multi-objective fitness function that determines the optimal positions and ratings of DERs has been developed. It is concerned with the total running and actual power failure, as well as the cost of construction and emissions dispatched via the grid. This multi-objective stochastic optimization problem is formulated using (1).

$$Minimization\ MOF = w1 \times \underbrace{\left(C_p + PV_{instt} + PV_{O\&M} + W_{instt} + W_{O\&M} + \sum_{t=1}^{24} C_{EV}(t)\right)}_{Total\ Cost} + w2 \times \underbrace{\sum_{t=1}^{24} P_{TLoss}(t)}_{Power\ Loss} + w3 \times \underbrace{\sum_{t=1}^{24} E_{EMSN}(t)}_{Emission} \quad (1)$$

where the primary term of a target function is the grid-purchased actual power cost (C_p), which can be expressed as a linear function using (2) [18].

$$C_p = \sum_{y=1}^{yr} PW^y \times 365 \times \sum_{t=1}^{24} \rho_E(t) \times P_{real}(t) \quad (2)$$

where PW is the present worth and is specified as $PW = (1 + \text{inf}R)/(1 + \text{int}R)$, with yr denoting the number of years. The PVGS (PV_{instt}) installation cost is denoted by the subsequent term of the target function and is exploited using (3). The third concept is the cost of PVGS operation and maintenance (PVO&M) [19][20], which is calculated using (4).

$$PV_{instt} = PV_{out} \times CP_{PV} \quad (3)$$

$$PV_{O\&M} = \sum_{y=1}^{yr} PW^y \times 0.03 \times PV_{instt} \quad (4)$$

The fourth term of the fitness function represents the WTGS (Winstt) installation cost, which is calculated using (5). WTGS O&M expense [19][20] is the fifth expression, and it is assessed using (6).

$$W_{instt} P_w \times CP_w \quad (5)$$

$$W_{O\&M} = \sum_{y=1}^{yr} PW^y \times 0.01 \times W_{instt} \quad (6)$$

The sixth term reflects the expense of charging and discharging electric vehicles (EVs) from and to the grid [21][22]. Vehicle owners should schedule the discharging/charging of their vehicles to ensure the best results. This could be described as

$$C_{EV}(t) = \rho_E(t)[\eta_{dch}P_{dch}(t) - \eta_{ch}P_{ch}(t)] \quad (7)$$

The seventh term of the fitness function is the summing of active power loss (P_{TLoss}) occurring over 24 hours across each branch of the distribution system. This is formulated thus

$$P_{TLoss} = \sum_{\substack{i=1 \\ i \neq j}}^{j} P_{Loss}(i,j) \quad (8)$$

$$E_{EMSN} = \sum_{t=1}^{24} P_{real}(t) \times (CO_2 + NO_X + SO_2) \quad (9)$$

Operating Constraints

2.1. Load Flow Evaluation

The load requirement must be met by accumulating electricity from the grid, PVGS, WTGS, and EVs. It is expressed in the following way in (10):

$$\sum_{t=1}^{24} P_{real}(t) + \sum_{t=1}^{24} P_{WTGS}(t) + \sum_{t=1}^{24} P_{PVGS}(t) + \sum_{t=1}^{24} P_{dch}(t) = \sum_{t=1}^{24} P_{ch}(t) + \sum_{t=1}^{24} P_{Load}(t) + \sum_{t=1}^{24} P_{TLoss}(t) \quad (10)$$

2.2. Constraining for Voltage

The voltage amplitude of each bus must be between the maximum and minimum limits.

$$V_i^{\min} \leq V_i \leq V_i^{\max} \qquad i \in NB \quad (11)$$

2.3. Constraining for Current

The thermal loading of each delivery segment should be less than its rating value in order to maintain network stability.

$$I_{ij} \leq I_{Th}^{rated} \quad (12)$$

2.4. Constraining for EVs

To ensure device durability, the total number of gridable vehicles arriving every hour for charging/discharging purposes is considered fixed.

$$\sum_{t=1}^{24} EV(t) \leq N_{EV} \quad (13)$$

$EV(t)$ is the number of EVs connected to the system during a particular time period and N_{EV} is the maximum number of allowable EVs at any time.

2.5. State of EV Battery Charge

It is estimated that each gridable vehicle will store up to 90% of power and release up to 20% of the rated energy of the vehicle battery.

2.6. Charging/Discharging of EVs

It is implied in this analysis that car discharging and charging are not performed simultaneously.

When completing the DERs integration mission, a number of factors were taken into account:

- The test network being handled as if it were in a healthy state;
- The first bus being called a slack bus, with a voltage value of 1 p.u.;
- Harmonics not being present in this realistic rural delivery scheme.
- The shunt conductance and susceptance of each delivery segment being considered insignificant.

2.7. Voltage Variation

One of the most important indicators of power quality is bus voltage. The poor behavior of the device is shown by a significant disruption in the voltage amplitude. The average voltage deviation of each bus over a 24-hour period is calculated using (14).

$$V_{deviation} = \sum_{t=1}^{24} \sum_{i=1}^{NB} \frac{|V_{rated} - V_i|}{V_{rated}} \quad (14)$$

$$V_{max} \geq V_i \geq V_{min}$$

The maximum allowable voltage is denoted by V_{max}, and the minimum allowable voltage is denoted by V_{min}. V_{max} is 1.1 times the rated voltage, and V_{min} is 0.9 times the rated voltage.

3. DERS – DİSTRİBUTED ENERGY RESOURCES

These DERs, according to this study, play a critical role in energy networks through activity and generation. The delivery network uses these as DGs. Gridable vehicles are hybrid vehicles that are capable of integrating electric technology into the grid. EVs transfer electrical power to the grid at peak hours to meet peak demand requirements, and these vehicles can be charged up to a certain maximum limit during off-peak times of the system, thereby reducing the amount of emissions produced by thermal power plants and improving network efficiency.

Three different DER aggregators were considered in this analysis to inform the Distribution Management System (DMS). According to the information gathered from these aggregators, the DMS distributes electric power. The WTGS aggregator will use WTGS to compile information on wind power generation. A PVGS aggregator can collect data on solar power generation by PVGS in a similar manner. In the case of EVs, each vehicle owner would first register their vehicle with an EV aggregator for the purpose of charging and discharging. The EVs aggregator would then submit information to the owner of the vehicle regarding charging and discharging options based on the grid's load settings. With the latest infrastructure

and smart estimation methods, this study implicitly has the smart delivery method, which will provide certainty for service and accurate usage of these DERs. The numerical models of these DERs are discussed in the following sections.

3.1. PVGS Mathematical Model

The amount of power produced by a PV module is primarily determined by the solar irradiance concentration. They typically expect a binomial allocation for the hourly irradiance incident at a fixed spot, which is an array of two linear uni-modal distribution functions [23][24]. For both uni-modals, a beta Probability Density Function (PDF) is created, as shown below:

$$f_b(s) = \begin{cases} \frac{\Gamma(\alpha+\beta)}{\Gamma(\alpha)+\Gamma(\beta)} \times s^{(\alpha-1)}(1-s)^{(\beta-1)} & for\ 0 \le s \le 1,\ \alpha \ge 0,\ \beta \ge 0 \\ 0 & otherwise \end{cases} \quad (15)$$

The solar irradiance (kW/m^2) is denoted by s, and α and β are the parameters of the beta distribution function $f_b(s)$, which can be determined using (16) and (17).

$$\beta = (1-\mu_s) \times \left(\frac{\mu_s \times (1+\mu_s)}{\sigma_s^2} - 1\right) \quad (16)$$

$$\alpha = \frac{\mu_s \times \beta}{1-\mu_s} \quad (17)$$

The entire day is divided into 24 one-hour time periods in order to generate the PDF. Similar to the solar irradiance, each hour has its own PDF. The hourly μ_s and σ of the day are measured based on historical evidence. Per hour is assumed to have 20 states of s with a phase of 0.05 kW/m^2. The PDF of the μ_s and σ_s hour of the day with 20 states is calculated using s values of Equation 15. According to this, the processing power of PVGS (PV_{out}) for that particular hour is calculated using (18) [24].

$$PV_{out}(s) = N \times F_F \times V_y \times I_y \quad (18)$$

$$V_y = V_{oc} - V_k \times T_{cy} \quad (19)$$

$$I_y = s[I_{sc} + I_k(T_{cy} - 25)] \quad (20)$$

$$F_F = \frac{V_{MPT} \times I_{MPT}}{V_{OC} \times I_{SC}} \quad (21)$$

$$T_{cy} = T_A + s\left(\frac{N_{OT} - 20}{0.8}\right) \quad (22)$$

At any given time interval t, the cumulative predictable output power (EOP) of PVGS is calculated using (23).

$$EOP_{PV}(t) = \int_0^1 PV_{out}(s) \times f_b(s) ds \quad (23)$$

Table 1 shows the hourly mean and standard deviation of s.

Table 1: Details of Solar Irradiance [25]

Solar Irradiance (kW/m^2)					
Hour	μ_s	σ_s	Hour	μ_s	σ_s
6	0.0158	0.0196	12	0.7305	0.1510
7	0.1605	0.0332	13	0.6780	0.1283
8	0.3412	0.0658	14	0.5699	0.1011
9	0.5060	0.1002	15	0.4124	0.0765
10	0.6385	0.1319	16	0.2394	0.0446
11	0.7120	0.1551	17	0.0834	0.0230

This information is taken from the Tripoli area delivery system site in the Libyan province of Tripoli [25]. Figure 1 shows the probability distribution and EOP of solar irradiance for a full 24 hours of 20 states. Figure 2 shows the hourly output power provided by a single PV module.

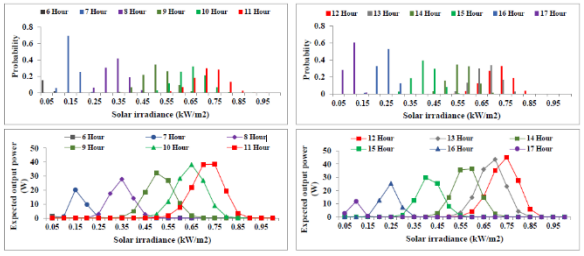

Figure 1: PDF and EOP values for each hour at various solar irradiance levels

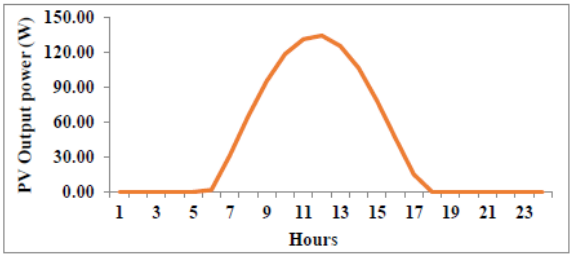

Figure 2: PV-module output control for each hour

3.2. Mathematical Model of WTGS

For each forecast moment, the widely used Rayleigh PDF is used to state the stochastic scenery of wind speed [5][26]. The form factor is set to 2 in this well-known case of the Weibull PDF:

$$f_w(v) = \left(\frac{2v}{c^2}\right) exp\left[-\left(\frac{v}{c}\right)^2\right] \quad (24)$$

where $f_w(v)$, c, and v are the Rayleigh PDF, scale factor and wind speed, respectively. The scaling factor c can be determined if the average wind velocity (v_m) is known (25 and 26).

$$v_m = \int_0^\infty v f_w \, dv = \int_0^\infty \left(\frac{2v^2}{c^2}\right) exp\left[-\left(\frac{v}{c}\right)^2\right] dv = \frac{\sqrt{\pi}}{2} c \quad (25)$$

$$c \cong 1.128 v_m \quad (26)$$

To create the PDF, the entire day was divided into 24 one-hour time periods, with each hour having its own PDF based on wind direction. The hourly μ_w and σ_w of the day was calculated using historical records. Every hour, 24 states of wind speed with a phase size of 1 m/s were considered. The PDF of each hour of the day with 24 states was calculated using μ_w and σ_w values (24). As a result, the output power of WT for that hour is calculated using (27). In addition, as seen in Table 2 [25], hourly dependent wind speed data were obtained from the Tripoli area delivery system site in the Libyan state of Tripoli.

Table 2: Details of wind speed [25]

Solar Irradiance (kW/m^2)					
Hour	μ_w	σ_w	Hour	μ_w	σ_w
1	9.900	0.7937	13	7.9667	0.3786
2	9.3667	0.8021	14	8.00	0.4583
3	9.1667	0.8505	15	8.00	0.500
4	9.000	0.8185	16	7.7333	0.4509
5	8.700	0.7550	17	6.9667	0.2309
6	8.600	1.0583	18	5.9667	0.3786
7	9.00	1.1533	19	4.8333	0.3215
8	9.0333	1.1504	20	4.4333	0.3215
9	9.3333	0.9504	21	4.3333	0.4163
10	9.600	1.1533	22	4.1000	0.2646
11	10.1333	1.0066	23	4.0667	0.2082
12	10.2667	0.8622	24	4.0000	0.1732

At any given time interval t, the cumulative EOP of WTGS is calculated using (28).

$$P_w(v) = \begin{cases} 0, & 0 \le v_{aw} \le v_{cin} \\ P_{rated} \times \frac{v_{aw} - v_{cin}}{v_{rt} - v_{cin}}, & v_{cin} \le v_{aw} \le v_{rt} \\ P_{rated}, & v_{rt} \le v_{aw} \le v_{cof} \\ 0, & v_{cof} \le v_{aw} \end{cases} \quad (27)$$

$$EOP_{WT}(t) = \int_0^1 P_w(v) \times f_w(v) dv \quad (28)$$

The EOP of *WT* for various wind speeds is calculated using Equations 24-28. Figure 3 shows the probability distribution and the EOP of the wind speed for each hour of the day for 24 states. Figure 4 also shows the hourly produced output power through WTGS.

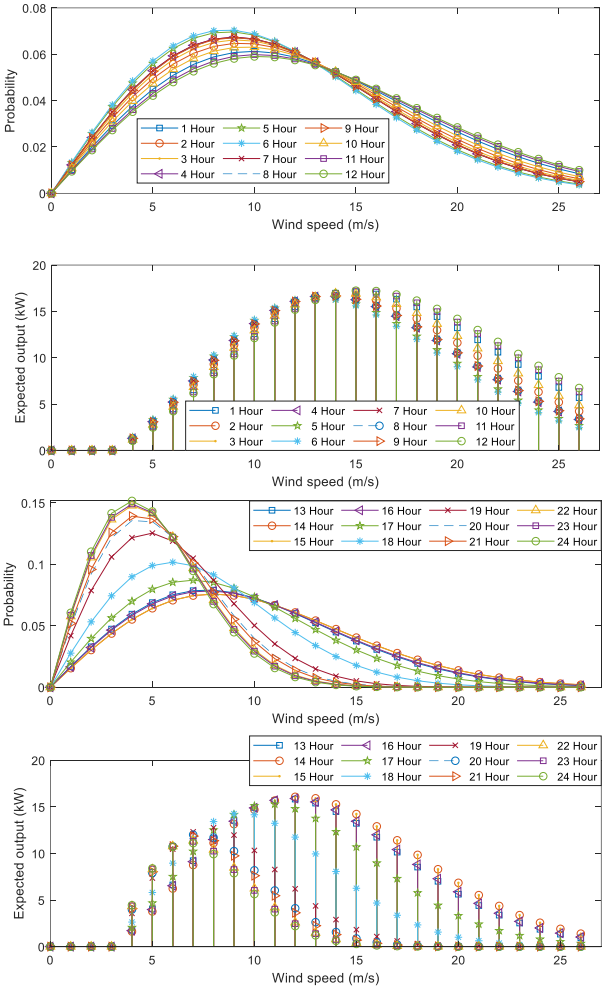

Figure 3: PDF values and EOP of each hour at various wind rates

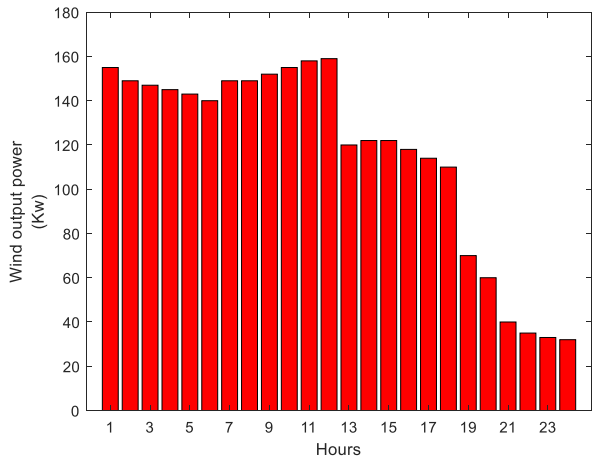

Figure 4: WT output power for each hour

3.3. Discharging/Charging Scheduling of EVs

Grid synchronized vehicles are used as a source to provide electricity to the grid during peak hours and for charging vehicles during off-peak hours of the grid in this study. According to the rules of the deregulated electrical energy industry, the spot electrical energy rate is announced one day ahead of time, and car owners settle on charging and charging schedules depending on this information [21][22]. Equations 29 and 30 are used to quantify the discharging/charging capacity of gridable vehicles over a 24-hour period.

$$P_{dch}(t) = \mu_{vcap}[\phi_{pre} - \phi_{min}]N_{Ev(dch)}(t) \quad (29)$$

$$P_{ch}(t) = \mu_{vcap}[\phi_{dep} - \phi_{pre}]N_{Ev(ch)}(t) \quad (30)$$

Here, ϕ_{pre} and ϕ_{dep} are the current and exit state of charge, $N_{Ev(ch)}$ / $N_{Ev(dch)}$ are the number of EVs arriving for charging or discharging, and μ_{vcap} is the battery capacity of an EV. The discharging/charging ratings of EV batteries should be held between the maximum (ϕ_{max}) and minimum (ϕ_{min}) levels for longer battery life.

$$\phi vcap_{vcap}\, vcap_{max}{}_{min} \quad (31)$$

3.4. Biomass Power Generation

Biomass is a combustible gas generated in the absence of oxygen through biodegradation reactions of organic matter from the activity of microorganisms and other causes, in natural media or in unique equipment (that is, in an anaerobic environment). Swamp gas is the name given to this kind of gas. Biomass is derived from agricultural waste, as plant waste degrades in a similar manner. Figure 5 shows biomass processing.

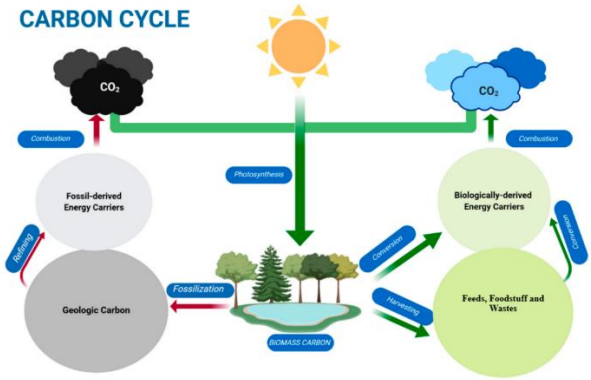

Figure 5: Processing of the biomass (extraction and use) [27]

The production of biomass occurs through anaerobic decomposition, which is a useful way to treat biodegradable waste since it produces a valuable fuel in addition to generating an effluent that can be applied as a soil conditioner or generic fertilizer.

As a result, the mixture contains methane in amounts ranging from 50% to 70% by volume, carbon dioxide, and lesser proportions of other substances such as hydrogen, phosphorus, oxygen, and hydrogen sulfide. Biomass has an average calorific value of between 18.8 and 23.4 MJ/m^3.

Libya's biomass capacity is small. Moreover, biomass energy sources are small and can only be used as a source of energy on an individual basis, thereby making it unsuitable for energy production [28]. The energy crisis in Libya's rural areas is acute, and new rural development is increasing demand for electricity, necessitating an assessment of the country's resources and environmental state. The universal use of biomass power generation technologies can be viewed as being ideal in rural areas where animal husbandry is an economic pillar industry and the region is rich in agriculture, forestry, and raw materials, promoting the growth of agriculture and animal husbandry, as well as farmer incomes.

The model follows a formula according to Equation 32 [29], with pressure and methane consumption as independent variables and the production capacity of the dependent variable as the dependent variable.

$$P_{BM} = \partial_0 + \partial_1 F_1 + \partial_2 F_2 + \partial_3 F_1^2 \quad (32)$$

where P_{BM} is the output power of biomass power generation in kW, F_1 and F_2 denote pressure (in kPa) and gas consumption (in Nm^3/h), respectively, ∂_0 denotes the constant; ∂_1 and ∂_2 are the pressure biomass power generation and gas consumption of linear coefficient, respectively, and ∂_3 is the quadratic term coefficient. The parameters obtained from the fitting function are shown in Table 3.

Table 3: Parameters used in biomass power generation

Parameter	Value
∂_0	2,338.10
∂_1	323.42
∂_2	8.46
∂_3	26.05

From Equations 7, 23, 28 and 32, the total power is calculated thus:

$$P_{Tot} = C_{EV}(t) + EOP_{PV} + EOP_{WT} + P_{BM} \quad (33)$$

After substituting Equations 7, 23, 28 and 32 into Equation 33, we have

$$P_{Tot} = \rho_E(t)[\eta_{dch}P_{dch}(t) - \eta_{ch}P_{ch}(t)] + \int_0^1 PV_{out}(s) \times f_b(s)ds + \int_0^1 P_w(v) \times f_w(v)d + \partial_0 + \partial_1 F_1 + \partial_2 F_2 + \partial_3 F \quad (34)$$

In this equation, P_{Tot} is the total power of these plants.

3.5. Cost, Power Loss and Emission Optimization

To determine elegantly any decision variable and ensure both equality and inequality constraints, an optimization approach was needed. The use of DERs should be maximized in order to reduce net costs, pollution and power loss to the bare minimum. This is only possible if the position and scale of DERs are accurately defined. As a result, the multi objective crow search optimization algorithm was used due to its robustness and ability to find the best result. Furthermore, under the unpredictable condition of both load and DERs, the optimal positions and quantity of DERs were calculated. As a result, they are regarded as decision factors and it is clear that this approach is appropriate and efficient to solve this hybrid nonlinear multi objective problem and achieve better results.

4. IMPLEMENTATION OF THE CSA ALGORITHM TO SOLVE THE OPTIMAL DERS INTEGRATION PROBLEM

The CSA optimization technique was used in this research to solve the optimum DERs installation challenge in order to minimize power loss, and overall expense (cost of purchase active power, WTGS installation, WTGS O&M, PVGS installation, PVGSO&M, EVs charging/discharging, and pollution generated by power plants). The best method to find a better solution that has been used in this case is as follows:

$$K^1 = [WT^1 \quad PV^1 \quad EV^1] \quad (35)$$

Here, K^1 is a vector. WT^1, PV^1 and EV^1 are the thirty-one column matrix, which may be expressed as

$$K^1 = \begin{bmatrix} \underbrace{WT^1_{loc1} \quad PV^1_{loc1} \quad PV^1_{loc2} \quad EV^1_{loc1}}_{Location\ of\ WT,\ PV\ \&\ EVs} \\ \underbrace{WT^1_{No.1} \quad PV^1_{No.1} \quad PV^1_{No.2} \quad EV^1_{No.1} \ldots\ldots EV^1_{No.24}}_{Number\ of\ WT,\ PV\ \&\ EVs} \end{bmatrix} \quad (36)$$

$$K^q = [WT^q \quad PV^q \quad EV^q] \quad (37)$$

The B/F load flow software is used to calculate the fitness function value for each and every qth solution. When the result value obtained is compared to the previous solution values, the healthier result is selected and the worse is discarded.

5. SİMULATİON RESULTS AND DİSCUSSİON

The effect of PVGS, WTGS, and EVs on a 28-bus delivery system is studied in this section. As a result, the suggested optimized solution to reduce overall expense, total power loss, and emissions was demonstrated on an 11 kV, 28-bus functional rural ring delivery feeder. This prototype structure has 28 vans, 27 branches, and a single primary delivery section with five sides. This machine has a base MVA of 100 and operates at 11 kV [28]. Figure 6 shows a single line representation of this test feeder. This test system can be found in the Kakdwip region (21.883°N 88.183°E) of West Bengal, India. It is linked to three types of clients, namely commercial, residential, and industrial, at various load buses [29][30]. Figure 7 shows the unpredictability of each bus's load requirement over a 24-hour period. Furthermore, the Indian Energy Exchange (IEX) [31] provides the hourly spot electricity market speed.

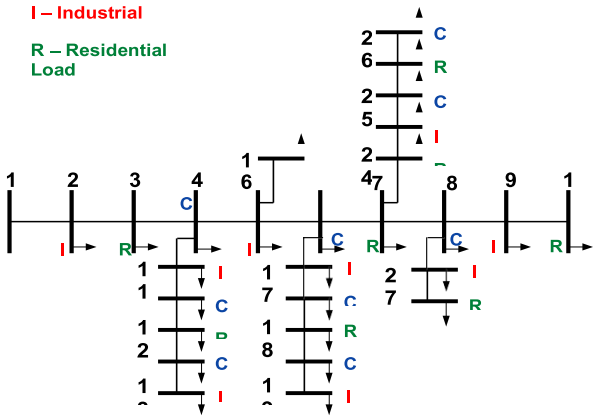

Figure 6: Functional radial delivery feeder for 28 buses.

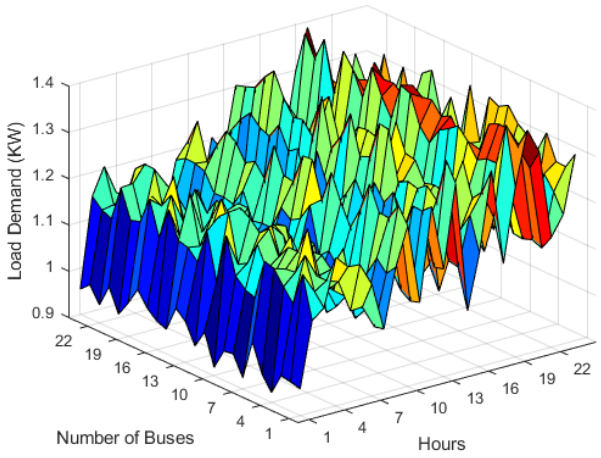

Figure 7: Load demand of each bus in the delivery network during a 24-hour period.

Renewable energy sources can run at a defined power factor that is closer to unity in relation to the electrical power network, according to the IEEE 1547 specification. Many electric power providers and independent power companies have determined that renewable energy sources will run at a limit of 0.95. In addition, different situations have been considered, as seen in Table 4, to assess the effect of renewable power sources by varying the power factor. Furthermore, the cost requirements for WTGS and PVGS that were used in this study were taken from [20]. WTGS, PVGS and EVs, on the other hand, are based on technological specifications from [20] and [32], respectively. This simulation was completed entirely in the MATLAB/Simulink platform (R2019a) version, which is compatible with Intel® CoreTM i7 processors. Furthermore, the following case-by-case exhaustive debates on simulation outcomes are discussed.

Table 4: Various cases for simulation analysis

Case	Explanation
1	Without any DERs integration (base case)
2	WTGS, PVGS, and EVs are optimally integrated into the delivery system. WTGS and PVGS have a leading power factor of 0.95.
3	WTGS, PVGS, and EVs are optimally integrated into the delivery system. At unity strength factor, WTGS and PVGS operate.
4	WTGS, PVGS, and EVs are optimally integrated into the delivery system. WTGS and PVGS have a lagging power factor of 0.95.

Table 5: Simulation results of all cases before and after DERs integration

Case	Case 1	Case 2	Case 3	Case 4
∑Ploss (kW)	554.55	419.70	348.57	225.81
% Ploss Reduction	-	24.32	37.14	59.28
∑Qloss (kVAr)	371.87	279.45	228.85	148.90
∑ Purchased real Power cost ($)	370,625,073.00	177,206,488.21	119,623,672.45	77,278,850.15
WT installation cost ($)	-	29,310,937.50	58,621,875	57,720,000.00
WTO & M cost ($)	-	41,528,029.36	83,056,058.72	81,778,273.20
PV installation cost ($)	-	7,361,640.00	24,555,960.00	74,891,520.00
PV O & M cost ($)	-	4,172,018.07	13,916,451.87	42,442,821.78
∑Emission (lb/kWh)	20,952.00	10,786.20	7,030.67	4,884.50

Case 1: This is the baseline scenario for the proposed evaluation system which excludes the use of DERs. The standard B/F load flow was used to calculate the feeder's active and reactive power loss, bus voltage, and line current value. As seen in Table 5, the reactive and active power losses of this test feeder are 371.87 kVAr and

554.55 kW, respectively. Furthermore, the cost of active power procurement from the grid is US$370,625,073.00, which corresponds to 20,952.00 lb/kWh of emissions dispatched via the power plant.

Case 2: In this case, both PVGS and WTGS, which are green power sources, inject active power and capture reactive power into and out of the network. These DERs are set up in the delivery system at the optimal allocations at the same time. The best position and ranking of WTGS are bus number 4 and one 250 kW unit, respectively. Similarly, the best location and PVGS ranking are bus number 5 and 62.92 kW, respectively. Bus number 6 is the best bus for charging and discharging electric vehicles. Figure 8(a) shows the PVGS produced production power hour by hour. Figure 8(b) shows the number of vehicles arriving for charging or discharging. Table 5 shows the simulation results obtained after the integration of DERs. Total power loss is reduced by 24.32%, with reactive and active power losses of 279.45 kVAr and 419.70 kW, respectively. Furthermore, the cost of grid-purchased actual electricity is US$177,206,488.21. The cost of installing WTGS and maintaining it is US$29,310,937.50 and US$41,528,029.36, respectively. Similarly, the costs of PVGS installation and operation and maintenance are US$7,361,640.00 and US$4,172,018.07, respectively. The amount of emissions generated is significantly decreased, and it now stands at 10,786.20 lb/kWh. Furthermore, the CPU takes 5,359.23 seconds to find the fitness value, including the load flow program, when solving this problem.

Case 3: Both PVGS and WTGS, which are green power sources, inject active power into the network in this situation. Additionally, gridable vehicles are used for charging and discharging. When charging, these vehicles function as a load, but when discharging, they provide power to the grid and are handled as a DG. These DERs were placed optimally in the distribution grid using the CSA methodology in order to reduce overall expense, power loss and pollution generation levels simultaneously. The WTGS optimum bus and rating are 21 and two 250 kW units. Similarly, bus numbers 9 and 11 are ideal locations for PVGS, with respective ratings of 61.16 kW and 148.72 kW. PVGS-1 and PVGS-2 provided output power by the hour in Figure 8(c), and the number of gridable vehicles incoming for discharging/charging is seen in Figure 8(d). The best bus for charging and discharging a vehicle's battery is bus number 16. These gridables may be discharged or charged at any moment, but not both at the same time. The concept of vehicle power generation at each hour is produced haphazardly, with a range of 1 to 100. Table 5 shows the simulation results after DER integration in this sense. Real and reactive power losses all decreased significantly to 348.57 kW and 228.85 kVAr, respectively. The decline in overall power loss is 37.14%. Furthermore, as compared to Case 1, the voltage level of each bus is significantly increased.

In the cost analysis section, integrating DERs reduces the cost of purchasing active power across the grid by a considerable amount, reducing it to US$119,623,672.45. WTGS installation and operation and maintenance costs are US$58,621,875 and US$83,056,058.72, respectively. PVGS installation and operation and maintenance costs are US$24,555,960.00 and US$13,916,451.87, respectively. The CPU computing time to find the solution value, including the load flow software, is approximately 4,379.50 seconds.

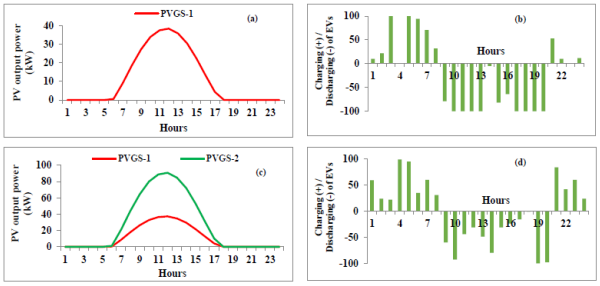

Figure 8: (a) PVGS-1 provided output power hourly for Case 2; (b) For Case 2, vehicles arrive every hour for charging/discharging; (c) PVGS-1 and PVGS--2 provided output power hourly for Case 3; (d) For Case 3, vehicles arrive every hour for charging/discharging.

Case 4: PVGS and WTGS both pump active and reactive power into the delivery feeder in this situation. WTGS's best location and rank is bus number 6, which has two 250 kW units. Similarly, PVGS's optimal positions are 11 and 22, with corresponding ratings of 340.12 kW and 309.98 kW on these buses. Bus number 2 is the best bus to charge and discharge electric vehicle batteries. PVGS provided output power by the hour and the number of vehicles arriving for charging/discharging purposes by the hour are depicted in Figures 9(a) and 9(b). Table 5 summarizes the numerical results in detail. The actual and reactive power losses after DER integration are 225.81 kW and 148.90 kVAr, respectively. The overall power loss has been reduced by 59.28%. Furthermore, as compared with other situations, the voltage level of each bus is greatly increased. Figure 10 shows a comparison of the voltage profile of each bus on an hourly basis for Case 4. The cost of purchasing active power from the grid is decreased significantly in the cost analysis section, and it now stands at US$77,278,850.15. WTGS installation and operation and maintenance costs are US$57,720,000.00 and US$81,778,273.20, respectively. PVGS installation and operation and maintenance costs are US$74,891,520.00 and US$42,442,821.78, respectively. Furthermore, for 100 loops, including the load flow program, the CPU measurement period to find the optimum fitness function value is approximately 4,449.13 seconds.

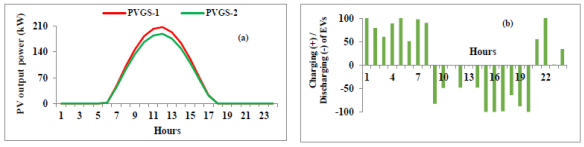

Figure 9: (a) PVGS-1 and PVGS-2 provided output power hourly for Case 4; (b) For Case 4, vehicles arrive every hour for charging and discharging.

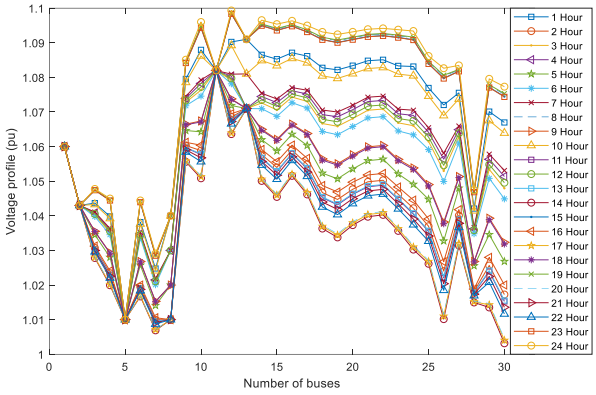

Figure 10: Voltage profile of Case 4 over 24 hours.

Following the integration of DERs, the hourly effect on the delivery network was also examined for each event. Figures 11(a) and 11(b) show the contrast of actual and reactive power losses in both situations. Figures 11(c) and 11(d) show the active power purchasing cost and voltage variance for each case over a 24-hour period, respectively.

When comparing the numerical outcomes of the different test cases, it is clear that Case 4 produces the best results.

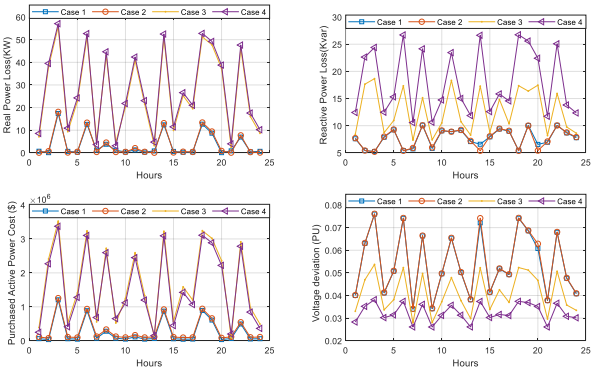

Figure 11: (a) Active power loss over 24 hours after DERs integration; (b) Reactive power loss over 24 hours after DERs integration; (c) Purchase active power cost from grid over 24 hours after DERs integration; (d) Voltage deviation over 24 hours after DERs integration

6. CONCLUSION

The effects of DERs on the delivery chain as a whole have been investigated. The gross costs, power losses, voltage variances, pollution levels, and electricity costs of the EVs are all decreased significantly after DERs integration. The probability values of wind speed and solar irradiance for each hour have been successfully evaluated using PDF. These probabilities can be used to calculate the EOP. Then, based on that, we determine the optimal number of WT units and PV modules. Renewable energy sources were used in this study with various power factors, such as unity and 0.95 lagging/leading. The research network seems to provide improved results when these green power sources are run at a 0.95 lagging power factor. With EVs, vehicle owners' successes in discharging/charging their EVs for financial benefits can increase load demand during grid off-peak hours. The CSA algorithm simulation results are professional and satisfactory in solving more common optimization tasks. It was also discovered that the algorithm is reliable and capable of finding the best answer in a limited number of cycles.

ACKNOWLEDGEMENT

The authors to be thankfull from Karabuk unıversıty to supportıng of thıs work.

DECLARATION OF ETHICAL STANDARDS

The author(s) of this article declare that the materials and methods used in this study do not require ethical committee permission and/or legal-special permission.

AUTHORS' CONTRIBUTIONS

Abdulbari Ali Mohamed FREI: Perofrmed the experiments and analyse the results.

Muhammet Tahir GÜNEŞER: Perofrmed the checking and modifiying the paper.

CONFLICT OF INTEREST

There is no conflict of interest in this study.

REFERENCES

[1] P. A. Boot and B. Van Bree, *A zero-carbon European power system in 2050: proposals for a policy package*. ECN, Energy research Centre of the Netherlands, (2010).

[2] K. Parks, P. Denholm, and T. Markel, "Costs and emissions associated with plug-in hybrid electric vehicle charging in the Xcel Energy Colorado service territory," National Renewable Energy Lab.(NREL), Golden, CO (United States), (2007).

[3] B. M. Marshall, J. C. Kelly, T.-K. Lee, G. A. Keoleian, and Z. Filipi, "Environmental assessment of plug-in hybrid electric vehicles using naturalistic drive cycles and vehicle travel patterns: A Michigan case study," ***Energy Policy***, 58; 358–370, (2013).

[4] J. Senthil kumar, S. Charles Raja, D. Srinivasan, and P. Venkatesh, "Hybrid renewable energy-based distribution system for seasonal load variations," ***Int. J. Energy Res.***, 42(3); 1066–1087, (2018).

[5] D. K. Khatod, V. Pant, and J. Sharma, "Evolutionary programming based optimal placement of renewable

distributed generators," ***IEEE Trans. Power Syst.***, 28(2); 683–695, (2012).

[6] Y. M. Atwa and E. F. El-Saadany, "Probabilistic approach for optimal allocation of wind-based distributed generation in distribution systems," ***IET Renew. Power Gener.***, 5(1);79–88, (2011).

[7] A. Şahinoğlu and M. Rafighi, "Machinability of hardened AISI S1 cold work tool steel using cubic boron nitride," ***Sci. Iran.***, 28; 2655–2670, (2021).

[8] A. H. Abed, J. Rahebi, and A. Farzamnia, "Improvement for power quality by using dynamic voltage restorer in electrical distribution networks," in ***2017 IEEE 2nd International Conference on Automatic Control and Intelligent Systems (I2CACIS)***, 122–127, (2017).

[9] A. Şahinoğlu and M. Rafighi, "Investigation of tool wear, surface roughness, sound intensity and power consumption during hard turning of AISI 4140 using multilayer-coated carbide inserts," ***J. Eng. Res.***, 9(4B); (2021).

[10] A. H. Abed, J. Rahebi, H. Sajir, and A. Farzamnia, "Protection of sensitive loads from voltages fluctuations in Iraqi grids by DVR," in ***2017 IEEE 2nd International Conference on Automatic Control and Intelligent Systems (I2CACIS)***,144–149, (2017).

[11] A. Şahinoğlu, M. Rafighi, and R. Kumar, "An investigation on cutting sound effect on power consumption and surface roughness in CBN tool-assisted hard turning," ***Proc. Inst. Mech. Eng. Part E J. Process Mech. Eng.***, 09544089211058021, (2021).

[12] M. RAFİGHİ, "Comparison of ceramic and coated carbide inserts performance in finish turning of hardened aisi 420 stainless steel," ***Politek. Derg***.

[13] M. T. Guneser, "Algorithms to Model and Optimize a Stand-Alone Photovoltaic-Diesel-Battery System: An Application in Rural Libya," ***Teh. Vjesn.***, 28(2); 523–529, (2021).

[14] A. Tabak, M. Özkaymak, M. T. Güneşer, and H. O. Erkol, "Optimization and evaluation of hybrid PV/WT/BM system in different initial costs and LPSP conditions," ***Optimization***, 8(11); (2017).

[15] A. Elbaz and M. Güneser, "Multi-objective Optimization of Combined Economic Emission Dispatch Problem in Solar PV Energy Using Hybrid Bat-Crow Search Algorithm," ***Int. J. Renew. Energy Res.***, 11(1), 383–391, (2021).

[16] A. A. M. Nureddin, J. Rahebi, and A. Ab-BelKhair, "Power Management Controller for Microgrid Integration of Hybrid PV/Fuel Cell System Based on Artificial Deep Neural Network," ***Int. J. Photoenergy,*** (2020).

[17] A. Ab-BelKhair, J. Rahebi, and A. Abdulhamed Mohamed Nureddin, "A Study of Deep Neural Network Controller-Based Power Quality Improvement of Hybrid PV/Wind Systems by Using Smart Inverter," ***Int. J. Photoenergy***, (2020).

[18] M. Dixit, P. Kundu, and H. R. Jariwala, "Incorporation of distributed generation and shunt capacitor in radial distribution system for techno-economic benefits," ***Eng. Sci. Technol. an Int. J.***, 20(2); 482–493, (2017).

[19] V. Black, "Cost and performance data for power generation technologies," ***Prep. Natl. Renew. Energy Lab.***, (2012).

[20] A. Maleki, M. G. Khajeh, and M. Ameri, "Optimal sizing of a grid independent hybrid renewable energy system incorporating resource uncertainty, and load uncertainty," ***Int. J. Electr. Power Energy Syst.***, 83; 514–524, (2016).

[21] W. Hu, C. Su, Z. Chen, and B. Bak-Jensen, "Optimal operation of plug-in electric vehicles in power systems with high wind power penetrations," ***IEEE Trans. Sustain. Energy***, 4(3); 577–585, (2013).

[22] A. Y. Saber and G. K. Venayagamoorthy, "Resource scheduling under uncertainty in a smart grid with renewables and plug-in vehicles," ***IEEE Syst. J.***, 6(1), 103–109, (2011).

[23] D. Q. Hung, N. Mithulananthan, and K. Y. Lee, "Determining PV penetration for distribution systems with time-varying load models," ***IEEE Trans. Power Syst.***, 29(6); 3048–3057, (2014).

[24] J.-H. Teng, S.-W. Luan, D.-J. Lee, and Y.-Q. Huang, "Optimal charging/discharging scheduling of battery storage systems for distribution systems interconnected with sizeable PV generation systems," ***IEEE Trans. Power Syst.***, 28(2), 1425–1433, (2012).

[25] P. Kayal and C. K. Chanda, "A multi-objective approach to integrate solar and wind energy sources with electrical distribution network," ***Sol. Energy***, 112; 397–410, (2015).

[26] G. Boyle, "Renewable energy," *Renew. Energy, by Ed. by Godfrey Boyle, pp. 456. Oxford Univ. Press. May 2004. ISBN-10 0199261784. ISBN-13 9780199261789*, p. 456, (2004).

[27] I. Ahmed *et al.*, "Socio-Economic and Environmental Impacts of Biomass Valorisation: A Strategic Drive for Sustainable Bioeconomy," ***Sustainability***, 13(8); 4200, (2021).

[28] O. Ramelli, S. Saleh, and J. Stenflo, "Prospects of renewable energy in Libya," in *International Symposium on Solar Physics and Solar Eclipses (SPSE), Tripoli*, (2006).

[29] S. Liang and J. Zhu, "Dynamic Economic Dispatch of Microgrid with Biomass Power Generation," in ***2017 6th International Conference on Energy and Environmental Protection (ICEEP 2017),*** (2017).

[30] W. W. Price, C. W. Taylor, and G. J. Rogers, "Standard load models for power flow and dynamic performance simulation," ***IEEE Trans. power Syst.,*** 10(CONF-940702-), (1995).

[31] E. Lopez, H. Opazo, L. Garcia, and P. Bastard, "Online reconfiguration considering variability demand: Applications to real networks," ***IEEE Trans. Power Syst.***, 19(1); 549–553, (2004).

[32] A. Ellis *et al.*, "Reactive power interconnection requirements for PV and wind plants–recommendations to NERC," ***Sandia Natl. Lab. Albuquerque, New Mex.***, 87185, (2012).